



**MONTCLAIR STATE**  
UNIVERSITY

Montclair State University  
**Montclair State University Digital  
Commons**

---

Theses, Dissertations and Culminating Projects

---

5-2023

**Antarctic Peninsula Ice Sheet Dynamics in the Pliocene from  
Sedimentological Interpretation of Ocean Drilling Program Site  
1097**

Ridley Joseph

Follow this and additional works at: <https://digitalcommons.montclair.edu/etd>



Part of the [Earth Sciences Commons](#), and the [Environmental Sciences Commons](#)

---

### **Abstract**

Studying ice sheet behavior during the Pliocene Epoch is of great importance. The Early Pliocene was characterized by warm climatic conditions, similar carbon dioxide levels and high sea levels compared to the present. This time frame provides essential information on the foreseeable future of Earth's cryosphere, particularly if climate change continues to persist. The sedimentary record of the Antarctic Peninsula Ice Sheet (APIS) is the focus of this study. At Ocean Drilling Program (ODP) Site 1097, cores were drilled into Pliocene strata at a shallow depth on the Antarctic Peninsula continental shelf. Sedimentary facies were interpreted, and twenty samples were selected and examined using laser particle size analysis and major and trace element geochemistry. The results provide evidence of glacial advance and retreat during the Early Pliocene. Sedimentary facies, particle size data, and bulk geochemistry support a persistent but dynamic APIS during this time. The data do not support the previous notion, based on ice-sheet modeling, that the Antarctic Peninsula could have been ice-free under warm Pliocene conditions. The lower part of the Pliocene section at Site 1097 shows evidence of ice distal sedimentary facies, whereas overlying Pliocene strata suggests that the APIS may have been a fully grounded ice sheet on the outer continental shelf, with facies attributed to subglacial environments. The low chemical index of alteration (CIA) values of the sediments point to a cool, dry climate and sediment with a strong glacial imprint. No significant changes in the source material are shown by trace and Rare Earth Element (REE) ratios.

MONTCLAIR STATE UNIVERSITY

Antarctic Peninsula Ice Sheet Dynamics in the Pliocene from Sedimentological  
Interpretation of Ocean Drilling Program Site 1097

by

Ridley Joseph

A Master's Thesis Submitted to the Faculty of  
Montclair State University

In Partial Fulfillment of the Requirements

For the Degree of

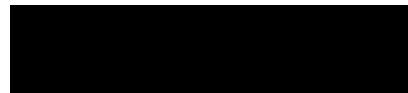
Master of Science

May 2023

College of Science and Mathematics

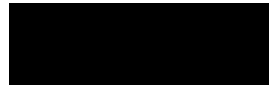
Department of Earth and  
Environmental Studies

Thesis Committee



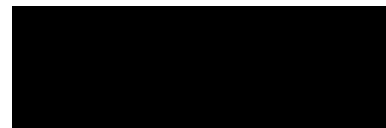
Dr. Sandra Passchier

Thesis Sponsor



Dr. Ying Cui

Committee Member



Dr. Matthew Goring

Committee Member

ANTARCTIC PENINSULA ICE SHEET DYNAMICS IN THE PLIOCENE FROM  
SEDIMENTOLOGICAL INTERPRETATION OF OCEAN DRILLING PROGRAM SITE 1097

A THESIS

Submitted in partial fulfillment of the requirements

For the degree of Master of Science

by

Ridley Joseph

Montclair State University

Montclair, NJ

2023

Copyright@2023 by Ridley Joseph. All rights reserved.

### **Acknowledgements**

I first need to extend gratitude to my thesis sponsor, Dr. Sandra Passchier, for being so much more than a research advisor during my time at Montclair. Thank you for believing in my potential based on just a few emails and a grad school application. Many of the opportunities I've had at MSU would not have been possible if not for you; thank you for the guidance, the advice, the support, and for always having an open door (even when it's closed). This project was partially funded from National Science Foundation award number OPP 2114839.

To Dr. Ying Cui, for agreeing to serve on my committee despite the abundance of responsibilities that come with a new position as Assistant Professor. Your expertise and genuine interest in your students are so appreciated. And to Dr. Matthew Goring, for guiding me through the majority of my academic career since undergrad. The quality of this research would not be as refined if it was not for you. Of course, a huge thank you to my predecessors whose research I cited, to propel my thesis to the next level.

## Contents

Abstract .....	1
Acknowledgements.....	5
Contents .....	6
List of Figures.....	7
INTRODUCTION .....	8
Background.....	8
Study Area .....	12
METHODOLOGY .....	13
Materials and Methods.....	13
Particle Size Preparation and Data Acquisition .....	14
Sample Preparation and Data Acquisition Using ICP-MS .....	15
RESULTS .....	16
Sedimentary Facies .....	16
Particle Size Analysis .....	17
DISCUSSION .....	18
Geochemistry and sediment provenance .....	18
Chronostratigraphy .....	22
Glacial Dynamics.....	22
Other Reconstructions of the Pliocene APIS .....	27
CONCLUSION.....	28
DATA STATEMENT.....	30
REFERENCES .....	39

**List of Figures**

Figure 1	Sedimentary facies associated with an Antarctic ice shelf (Hambrey <i>et al.</i> , 1991).	31
Figure 2	ODP Site 1097 studied in this thesis is located at the seaward end of Marguerite Trough, Antarctica (Barker <i>et al.</i> , 1999).	32
Figure 3	Geological map of the Antarctic Peninsula, showing the distribution of the principal geological units defined in the text (Burton-Johnson & Riley, 2015).	33
Figure 4	Interpreted Core section IODP Site 1097 Leg 178 lithofacies for Cores 25R through 37R (Barker <i>et al.</i> , 1999).	34
Figure 5	Grain Size Distribution of 20 core samples. The horizontal axis refers to particle diameter in micrometer. The vertical axis shows volume percent in each half Phi bin.	35
Figure 6	Median grain size ( $\mu\text{m}$ ) with depth in meter below sea floor (mbsf).	35
Figure 7	The silt to clay ratio of all 20 samples studied.	36
Figure 8	Uniformity is indicated on the x axis and y axis core depth in meters below the seafloor calculated as the diameter greater than that of 60% of particles divided by the diameter greater than 10% of particles (Passchier <i>et al.</i> , 2018). The range is from 208.5-308.5 mbsf.	36
Figure 9	A plot of Th/Sc versus Zr/Sc ratio of the 20 samples taking from cores of IODP 1097 (McLennan <i>et al.</i> , 1993).	37
Figure 10	Plot of GdN/YbN versus Eu/Eu* ratio of the 20 samples that were examined from ODP Site 1097 (McLennan <i>et al.</i> , 1993).	37
Figure 11	Th/U versus Th plot ratio of 20 samples that were examined from Site IODP Site 1097 (McLennan <i>et al.</i> , 1993).	38
Figure 12	The vertical axis is CIA values of samples of IODP 1097, and the horizontal axis pertains to mbsf of each sample.	38



## INTRODUCTION

### Background

The Antarctic Peninsula ice sheet (APIS) is very dynamic and has increased sensitivity to climate change, compared with other ice sheets located on the continent. Sediment records show that the Antarctic Peninsula warms at a significantly faster rate than the rest of Antarctica (Davies *et al.*, 2012). Currently, the APIS is experiencing significant environmental changes because of increased global temperatures (Cook *et al.*, 2005). These changes are inducing rapid glacial retreat throughout the entire peninsula, leading to potential ice shelf collapse. Therefore, it is crucial to observe and compare these conditions to similar paleoenvironments (Davies *et al.*, 2012) in order to understand the key processes that are controlling ice sheet advance and retreat on the Antarctic Peninsula.

During the Pliocene (5.3 -2.6 Ma), the carbon dioxide levels were very similar to the present. However, the global temperature was approximately 2-3°C higher than it is today (Crampton-Flood *et al.*, 2018). This study aims to investigate the marine and terrestrial geological records of the Antarctic Peninsula during the Early Pliocene to gain a better understanding of ice sheet dynamics in periods of prolonged temperatures slightly higher than the present. This will enable us to project the future of the APIS and its effects on environmental conditions. The project will employ facies interpretations to reconstruct the depositional environments, particle size analysis and inductively coupled plasma-mass spectrometry (ICP-MS) to reveal evidence of ice shelf collapse and glacial-interglacial cyclicity.

Ice sheets located below sea level in Antarctica and grounded on the ocean floor are highly vulnerable to climate change due to the changing ocean currents (Prothro *et al.*, 2018) and the intrusion of circumpolar deep water (CDW). The CDW is a water mass originating from the

Pacific and Indian Oceans, becoming mixed with Antarctic water masses in the Southern Ocean. It is one of the significant contributors to the melting of ice shelves in the Antarctic region (Smith *et al.*, 2019). The grounding line, which is the seaward point of an ice sheet, is well known to be the tipping point of ice sheet stability (Reese *et al.*, 2022). To gain insight into the behavior of ice sheets, the sedimentary record is the most informative compared to satellite and airborne remote sensing and ice-penetrating radar surveys. Sediment cores provide detailed information about glacial extent, primary productivity and oceanic processes, surpassing landforms, which only provide a record of the last deglaciation (Prothro *et al.*, 2018). Consequently, sediment cores are the primary source of investigation for the dynamics of the APIS.

According to Barker *et al.* (2002), the Antarctic Peninsula region and its ice sheet are thought to be particularly sensitive to climatic change. The Antarctic Peninsula has warmed over the past 50 years far more quickly than the rest of Antarctica, according to observational records (Vaughan *et al.*, 2003). Despite the mounting evidence of ice-sheet instability, very little is known about the extent and thickness of the APIS during prolonged warm periods. Therefore, one of the objectives of this study is to address this knowledge gap. This study would provide a deeper understanding of the potential impact of climate change on the APIS (Smellie *et al.*, 2009). Studying the APIS provides essential information regarding the destabilization of ice sheets and ice shelves.

Over the last ten million years, the APIS has exhibited an extensive history of advance and retreat. However, during the Pliocene, it remains unclear if the APIS retreated near its current position or disappeared entirely during interglacials (Smellie *et al.*, 2009). A relevant study conducted on James Ross Island, situated off the coast of the Antarctic Peninsula,

investigated the stratovolcano named Mt. Haddington, which is a primary source of the rich basalt lava flows located on the island (Johnson *et al.*, 2009). The basalt lava flows dated at 4.69 Ma were ideal for performing cosmogenic  $^3\text{He}$  exposure dating, which helped in answering various questions, including the extent of ice coverage and thickness of the APIS during the Pliocene. Samples obtained from Crisscross Crags and Patalamon Mesa indicated minimal exposure to cosmic rays. Specifically, the exposure to cosmic rays was restricted to 15 kyr, meaning that the sample location was exposed for only that duration within the last 4.69 Myr indicating that thick snow or ice engulfed this section of James Ross Island for an extended period. The samples were collected at an altitude above 600 m above sea level, suggesting that the APIS was at least 600 m thick for much of the last 4.69 Myr (Johnson *et al.*, 2009).

Field samples show contrasting results with the Pliocene ice-sheet conditions modeled by DeConto and Pollard (2016). An atmospheric regional climate model (RCM) and global climate model were used, coupled to an Antarctic ice sheet model. The ice sheet model depicted essential details about ice shelves and ice sheet margins since grounding line dynamics depend on the atmosphere and ocean. When buttressing is lost and retreating grounding zones widen, ice-shelf retreat can exceed its dynamically accelerated seaward flow in the presence of sufficient atmospheric warming above or ocean warming below (Shepherd *et al.*, 2004). The Pliocene model simulation in DeConto and Pollard (2016) was associated with  $\text{CO}_2$  level of 400 ppm, a warm summer orbit, and a 2 °C increase in ocean temperature, which represented the peak of the Pliocene warmth. These conditions resulted in an 11.3 m rise in global sea levels, partly caused by a major ice sheet retreat mainly due to melt and hydrofracturing of ice shelves, which are a primary reliever of back stress for an ice sheet. Marine ice sheet instability was detected all around the continent, including East Antarctica, West Antarctica, and the Antarctic Peninsula.

The model also predicted that if sea surface temperatures were warmer than 2° C, the Antarctic Peninsula would be ice-free (DeConto and Pollard, 2016).

The simulation provides a long-term perspective of current conditions in West Antarctica because the present and Pliocene climate are similar. However, none of the modeling work interprets the ice sheet dynamics compared with the observed sedimentary records of this area. Geological records can be used to reconstruct ice sheet dynamics, particularly grounding line dynamics. Even though there is limited insight into modern ice sheet dynamics since technology is not advanced enough to explore beneath ice sheets, recent scientific contributions to ice sheet, ice shelf, and grounding line dynamics have improved understanding of environmental changes in the Antarctic Peninsula (Prothro *et al.*, 2018; Smith *et al.*, 2019). The breakup of ice shelves caused by hydrofracture from water-filled crevasses has been linked to climate change (Smith *et al.*, 2019), and was also the driving force behind the ice sheet breakdown in the previously mentioned ice sheet model (DeConto and Pollard, 2016). Additionally, CDW upwelling, a crucial driver of ice shelf retreat today, could have also affected ice sheet dynamics during the Pliocene.

Lithofacies analysis of the continental shelf provides information about ice-proximal depositional environments through geological history. Examining cores from Pliocene strata at ODP Site 1097 may provide evidence of ice shelf collapse during a previous warm period. Glacial environments and geological signatures, such as subglacial, grounding line proximal, glacial distal, sub-ice shelf, calving zone, open marine, and ice shelf collapse, have been studied extensively and can be interpreted from unique sedimentary facies, ranging from massive diamictite to mud with dropstones (Figure 1). Evidence of sedimentary processes, including subglacial deformation till, proglacial sediment gravity flow, and open marine deposition, can be

found in the Pliocene strata at Site 1097 (Figure 2). However, geological imprints of ice shelves are still not well understood since the processes occurring in their vicinity are not clear (Smith *et al.*, 2019). Nevertheless, recent advances in understanding the geological signatures of ice shelves have been made since the lithostratigraphy of Site 1097 was last examined 20 years ago (Eyles *et al.*, 2001).

### **Study Area**

The Antarctic Peninsula, an extension of West Antarctica, spans about 1700 km from its southern to northern tip. In contrast to East Antarctica, the climate on the peninsula is relatively warm and wet (Smellie *et al.*, 2009). The majority of precipitation that occurs on the peninsula is in the form of snow due to its higher topography compared to other regions of Antarctica.

The APIS, the smallest and most northern extension of the Antarctic ice sheets, has an average thickness of 600 meters, which is relatively thin compared to the East Antarctic ice sheet that is over 2500 m thick. The Antarctic Peninsula covers approximately 521,790 km<sup>2</sup> and exhibits a climate similar to Greenland and Patagonia rather than the eastern part of the continent. Numerous studies have revealed that the Antarctic Peninsula is highly sensitive to climate change, evidenced by retreating ice sheets and ice shelf collapses (Cook *et al.*, 2005).

The Antarctic Peninsula boasts a diverse geology that can be categorized into six major rock units: the metamorphosed basement, Jurassic to Cenozoic sedimentary rocks, non-metamorphosed intrusive rocks, Paleozoic to Triassic sedimentary rocks, Jurassic to Paleogene volcanic rocks, and Neogene to recent alkaline rocks (Figure 3).

However, early on, all volcanic rocks on the Antarctic Peninsula were consolidated into the Antarctic Peninsula Volcanic Group, which failed to consider the diverse characteristics of the geology of the peninsula, such as tectonic setting, eruption age, or geochemistry. To address

this limitation, the Antarctic Peninsula Volcanic Group can be subdivided into two groups based on their compositions: Jurassic siliciclastic volcanic rocks and intermediate-mafic rocks. During the Jurassic period, volcanic activity was widespread, and the eastern section of Graham Land was the primary location for silica-rich ash deposition (see Figure 3). Later, the volcanism moved westward, and the magma from this volcanic activity eventually crystallized into granites (Burton-Johnson & Riley, 2015).

## METHODOLOGY

### Materials and Methods

Ocean Drilling Program (ODP) Leg 178 retrieved cores from two sites on the Antarctic Peninsula continental shelf: Site 1103 and Site 1097, as documented by Eyles *et al.* (2001). This study is focused on the records of ice sheet dynamics during the Early Pliocene, and Site 1097 was of particular interest due to its location at the seaward end of the Marguerite Trough (Eyles *et al.*, 2001), a major glacial outlet in West Antarctica. Although the top 150 meters of the cores were poorly recovered, the sediment became progressively more consolidated with depth, enabling scientists to interpret biofacies, lithofacies, and depositional environments (Eyles *et al.*, 2001). These cores contain microfossils such as foraminifera and radiolaria, providing a pristine record of late Cenozoic ice sheet growth. However, the methods and procedures used to analyze the cores in the past have been updated, and a more thorough investigation is necessary.

In this study, information from Site 1097 was obtained from the International Ocean Discovery Program website ([web.iodp.tamu.edu](http://web.iodp.tamu.edu)) and the Eyles *et al.* (2001) paper, as well as geological interpretations of the core and photo archives. To interpret depositional environments, the facies scheme of Smith *et al.* (2019) was employed for most of the retrieved portions of the core. However, some sections were complex and required analytical data of particle size and

trace elements for a more comprehensive understanding of the Pliocene period. Therefore, geochemical and grain size analyses were used to gain a better understanding of the sedimentary provenance and facies, as visual observations alone were insufficient. Sample selection was conducted by examining a visual archive of cores taken from site 1097, which ranged from sections 25R to 46R (Barker *et al.*, 1999). Sediment logs with sediment facies interpretation were also utilized for sample selection. Previous work done on Site 1097 aided in the final decision of sample selection. The core sections with the most variability were chosen for further analysis.

A total of 20 samples were taken from cores 26R, 27R, 28R, 32R, 33R, 34R, 35R, and 36R. The Malvern Mastersizer 3000 laser particle sizer was used to determine sediment mean size, sorting, and depositional environments. The Thermo Scientific iCap Q Inductively coupled plasma mass spectrometer (ICP-MS) was employed for chemical analysis to identify sediment provenance. All procedures and instrument analyses were conducted at Montclair State University.

### **Particle Size Preparation and Data Acquisition**

The samples for particle size analysis were prepared using the standard method outlined in Konert and Vandenberghe (1997). Subsamples were manually extracted from larger samples, and if necessary, a hammer was used to assist with separation. Approximately 0.5 cc of the subsample was placed in a 250 ml beaker and 10 ml of 30% hydrogen peroxide solution was added to remove any organic material present in the sediment. Millipore water was then added to the beaker until the volume reached approximately 50 ml. The solution was swirled to further promote sediment disaggregation, and then heated on a hot plate. After the reaction ceased, hydrochloric acid was added to dissolve any calcium carbonate present in the sample. Roughly half of the subsamples reacted with the solution, and the beakers were removed from the hot

plate once the sediments stopped reacting. The beakers were then cooled, and the samples were transferred to a 50 ml centrifuge tube and spun at 2000 rpm for 30 minutes. The supernatant was removed, the tubes were refilled with Millipore water and the centrifuge process was repeated. This process was conducted to remove any remaining hydrogen peroxide and hydrochloric acid, and to prepare the samples for measurement in the Malvern Mastersizer 3000 laser particle sizer. Before transfer to the laser particle sizer, samples were heated with Sodium Pyrophosphate to disperse aggregates.

Data collected on the Malvern Mastersizer 3000 was processed and exported using the instrument software, and analyzed using GRADISTAT (Blott and Pye, 2001). These programs generated graphs and calculated values that revealed details about the particle size distributions. The Malvern Mastersizer 3000 software provided information on the average mean grain size and uniformity of the samples, while GRADISTAT was used to calculate the sand to mud ratio and the sorting type of each sample. The dataset was then plotted on a sand-silt-clay ternary diagram, which helped clarify the depositional environments and determine the dynamics of the APIS.

### **Sample Preparation and Data Acquisition Using ICP-MS**

Sample preparation followed that of Murray *et al.* (2000). Twenty subsamples were ground to a fine powder with an alumina mortar and pestle. The subsamples were then weighed to  $0.1000\text{g} \pm 0.0005\text{g}$  and mixed with  $0.4000\text{g} \pm 0.002\text{g}$  of lithium metaborate flux on a weighing paper until they were completely mixed. The masses of the subsample and flux were recorded and then transferred to graphite crucibles. Crucibles were placed into a furnace at  $1050^\circ\text{C}$  for 30 minutes, creating a glass bead. Along with the subsamples, a blank with only 0.4g of lithium metaborate and no sample was inserted. The glass beads were then transferred to Teflon



beakers with 50 ml of 7% nitric acid with a magnetic stir bar, which assisted with the digestion of the bead into the acid solution. Once the bead was completely dissolved in the acid solution, it was then funneled with filter paper into a 60 ml bottle. This solution had a 500x dilution factor, which is a direct result of the preparation method.

The measurement of rare earth elements (REEs) and trace elements required further dilution due to the instrument's increased sensitivity to these components. To achieve this, 0.5 ml of the master solution was pipetted into a tube, and 9.5 ml of 2% nitric acid solution was added to achieve a dilution factor of 10,000x. The resulting test tubes, with a dilution factor of 10,000x, were inserted in a rack alongside 12 United States Geological Survey standards prepared using the same method as the 20 subsamples. These standards were crucial for generating calibration lines for each element. After every fourth sample, the instrument recorded readings from a drift solution. The raw data was converted into an Excel spreadsheet and adjusted for blank measurements and instrument drift.

## RESULTS

### Sedimentary Facies

The analysis of core images was facilitated by lithological information from Eyles *et al.* (2001) and the Site chapter (Shipboard Scientific Party, 1999), which aided in the characterization of sedimentary facies following the approach of Smith *et al.* (2019). The fossil assemblages in each section were classified into three biofacies (A, B, and C) based on the description of Eyles *et al.* (2001). Core sections composed only of gravel, where facies and environment could not be interpreted, were identified as 29R, 30R, 31R, 38R, 41R, and 43R (Figure 4).

The cores that showed the least variability were 25R, 28R, 37R, 39R, 40R, 42R, 44R, 45R, and 46R. The sediments in these cores were characterized by massive to stratified diamictite with occasional bioturbation, and Biofacies A to B. Biofacies A was described as poorly preserved, reworked assemblages of benthic foraminifera, while Biofacies B was a diverse assemblage of benthic foraminifera that occurred primarily in stratified and graded diamictite interbedded with bioturbated mudstones.

The cores that showed the most variability were 26R, 27R, 34R, 35R, 36R, and 44R. Core 34R exhibited the most variability, alternating between massive diamictite, burrowed diamictite, and massive mud. These facies can be interpreted as representing grounding line (GL) distal to open marine environments, which is distinct from the subglacial and GL proximal environments that were more prevalent in other sections. Core 27R also included an intriguing interval, containing large boulders interspersed with wavy and laminated silty clay.

Massive to stratified diamictite facies generally indicate subglacial and GL proximal environments but may also suggest an ice shelf collapse. To confirm the type of environment represented by these facies, particle size analysis and extensive visual analysis of the core are required. Subglacial and GL proximal facies typically indicate ice sheet advancement, which suggests a cooler climate, while ice shelf collapse facies suggest a warmer climate. Lastly, cores 34R, 35R, and 36R are distinct from the other sections examined, displaying open GL distal to open marine environments. Biofacies C is present in these cores, consisting of well-preserved foraminifera and other biogenic materials (Eyles *et al.*, 2001).

### **Particle Size Analysis**

The examination of core sections revealed variability in grain size distribution, as demonstrated by particle size data (Figure 5). Among the 20 samples examined, 15 had a

composition of sandy silt with varying sand content. Of these samples, three had a sand content over 20%, nine had a sand content over 10%, and three had a sand content over 5%. The remaining five samples, which were not sandy silt, had a mud content of 93% or greater and ranged from medium to coarse silt. All core samples were poorly to very poorly sorted sediment.

The average median grain size fluctuated throughout the core, with coarser sediments located at greater depths and finer sediments in shallower depths (Figure 6). The valleys on the graph or low peaks represent the deposition of very fine material, while the peaks are the deposition of larger particles (Figure 6). The fine materials are medium to coarse silt, and the coarse material is fine to very fine sand, representing the smallest and largest average particle sizes in this dataset.

A quantitative indication of grain sorting is uniformity, which is calculated as  $D_{60}/D_{10}$ , or the diameter greater than that of 60% of particles divided by the diameter greater than 10% of particles (Passchier et al., 2018). The uniformity of the dataset with an average value of 0.9 indicates that sediment became well-sorted with depth (Figure 8). The peak in the uniformity graph represents the most poorly sorted sample in the dataset and correlates to the lowest point on the average median grain size graph (Figure 6). Core section 33R is represented by the peak in the uniformity graph and the valley, or lowest point, in the average median grain size graph.

## **DISCUSSION**

### **Geochemistry and sediment provenance**

Bulk geochemical analysis via ICP-MS can be used for determining the provenance of sedimentary rocks and sediments. This technique sheds light on the extent of the APIS during the Pliocene. Even in small quantities, key trace elements are strong indicators of provenance. Fine-grained sediment or sedimentary rocks are usually a mixture of materials from various sources,

and the geochemical signature of these samples provides clues to the terranes and sedimentary processes that may have transported the sediment (McLennan *et al.*, 1993). Sands and mud can have different sources, and both may have opposing origins.

Th/Sc or Zr/Sc ratios are known to be strong indicators of igneous differentiation processes (McLennan *et al.*, 1993), with increasing Zr/Sc ratios commonly seen in turbidite sands in active margins. The Th/Sc versus Zr/Sc plot (Figure 9) in this study showed an upward trend in the Zr/Sc ratio, although the values were low overall. These low ratios reflect more of an active margin, which is not as strongly affected by sedimentary processes. High values would have suggested a trailing edge setting resulting from sedimentary sorting and recycling. The plot in Figure 9 suggests a simple relationship between the ratios of Th/Sc (average 0.37) and Zr/Sc (average 9.28) which is interpreted as compositional variants (McLennan *et al.*, 1993).

On chondrite-normalized diagrams, europium is frequently enriched (positive Eu-anomaly) or depleted (negative Eu-anomaly) in comparison to other REE. This can be measured using the expression  $Eu/Eu^*$ , where  $Eu^*$  is the anticipated europium value for a smooth chondrite normalized REE pattern (versus atomic number).

$$Eu/Eu^* = Eu_N / (Sm_N * Gd_N)^{0.5}$$

'N' stands for chondrite-normalized values in the equation above.

Archean turbidites typically exhibit higher  $Eu/Eu^*$  ratios, indicating that their metamorphic and igneous provenance was not significantly affected by intracrustal differentiation. They also tend to have  $Gd_N/Yb_N$  which reflects the ratio of fractionation of REE greater than 2.0, with high ratios of this sort being typically absent from post-Archean active margins. The  $Eu/Eu^*$  versus  $Gd_N/Yb_N$  REE diagram, showing the distribution of samples in Figure 10, shows the values of these ratios in the samples taken from IODP Site 1097, which do

not fall within these parameters. The samples had relatively low  $Gd_N/Yb_N$  values  $>1$  but  $<1.2$ , and low  $Eu/Eu^* <1$ , which is a strong indicator that the sediment was derived in post-Archean active margin settings, and intracrustal differentiation may have played a role in their provenance (McLennan *et al.*, 1993).

Another compelling plot was Th/U versus Th, which is known to correlate to modern turbidite muds from various tectonic settings (Guo *et al.*, 2012). The Th/U versus Th plot (Figure 11) shows a depletion of the ratios, which is commonly found in sediments in active margins. Furthermore, these depletions of Th occur due to enrichments of U because solubility and enrichment of U leads to fractionation of Th (Robinson *et al.*, 2009). Low values of Th and high U values are a strong indicator of depleted mantle sources for the arc provenance, as seen in Figure 11.

ICP-MS analysis of sediment from IODP Site 1097 revealed the geochemistry of intermediate rocks. Active margins typically show increasing Zr/Sc ratios, consistent with the Antarctic Peninsula's geology, which was an active continental margin magmatic arc 20 to 90 million years ago (Jordan *et al.*, 2020). In addition, the breakup of Gondwana could have played a significant role in this geochemistry signature. Most intermediate rocks found on the Antarctic Peninsula formed during the breakup of Gondwana, the supercontinent about 145 million years ago. This makes the source of sediments found at the site Late Jurassic to Early Cretaceous in age. Jurassic intermediate rocks are found throughout the peninsula, primarily in the eastern and central domains, with a small presence in the western domain of the peninsula (Burton-Johnson & Riley, 2015). The primary provenance of the sediment found in IODP Site 1097 is believed to be derived from the Chon Aike Volcanic Group and Graham Volcanic Group, large igneous provinces dominated by Jurassic volcanic rocks located in the eastern domain of the peninsula.

Nesbitt & Young (1982) established the Chemical Index of Alteration (CIA) as a way to quantify the contribution of chemical weathering to the formation of clastic deposits. The ratio  $CIA = (Al_2O_3 / (Al_2O_3 + CaO^* + Na_2O + K_2O)) \times 100$  (where  $CaO^*$  is the calcium content of silicates) is based on the presumption that feldspar degradation and clay mineral production constitute chemical weathering's primary processes. It can evaluate the degree of weathering and reveal key characteristics of an environment.

In this study, CIA was calculated on the 20 samples examined, and the values were found to be less than 55 (Figure 12). Environments with CIA values less than 60 are unlikely to have endured significant chemical weathering because the climate under which these values are observed in recent sediments is usually very cold and dry (Nesbitt & Young, 1982). A high CIA value is a strong indication of the removal of cations during weathering. A low CIA value indicates the absence of weathering or chemical alteration in the source area of the sediments, which usually suggests cold and arid environment (Fedo *et al.*, 1995).

Given that silt makes up a sizable portion (~ 70%) of samples and that CIA values are constantly within the glacial range, it is clear that the sediment retains a glaciogenic signature. According to Passchier *et al.* (2017), the silt fraction contains the majority of the detrital material associated with glacial erosion (also known as glacial rock flour). Clay minerals are prone to form when silt-sized minerals are exposed to a warm, humid atmosphere where chemical weathering is prevalent (Thiry, 2000). CIA values below 65 support the idea that pedogenic completion was not possible given the retention of the silt component in sediments. A relatively shallow depositional environment and severe physical weathering conditions are suggested by the low clay percentages.

### **Chronostratigraphy**

The age model of Eyles *et al.* previously restricted the studied interval to be within the 5.55 to 5.10 Ma range. However, the diatom zonations have since changed, and the *T. inura* zone attributed to Cores 26R-28R, previously defined as 5.55 Ma to 5.10 Ma, now stretches from about 4.85 Ma to 4.4 Ma (McKay *et al.*, 2019). The diatom assemblages in Cores 31R to 41R belong to the *T. oestrupi* zone dated between 5.5 and 4.85 Ma. Additionally, the uppermost parts of Cores 26R-28R belong to the lower quartile of the Upsilon radiolarian zone (4.6-3.6 Ma), while Cores 33R-36R belong to the Tau radiolarian zone (5.0-4.6 Ma)(McKay *et al.*, 2019). These age constraints suggest that the studied interval in Cores 36R-33R is dated to between ~5.0 and 4.85 Ma and the interval in Cores 28-26R to between 4.6 and 4.4 Ma.

### **Glacial Dynamics**

IODP Site 1097 was taken from the Antarctic Peninsula continental shelf. The sediments of Site 1097 display similarities to those of open marine and glacial distal environments, which are characterized by various features such as diatomaceous mud (open marine), dropstone mud (calving zone), sandy mud, or mud (sub-ice shelf and distal) that can result from rainout, ice rafting, marine plumes, and suspension settling (Barker *et al.*, 1999). These observations point toward a subpolar climate with warm summers and severe winters (Eyles *et al.*, 2001), which were most likely prevalent during the Early Pliocene on the Antarctic Peninsula.

The APIS underwent numerous ice volume fluctuations throughout the Cenozoic, and advances created ground zone wedges (GZW) (Bart & Andersen, 1997). Cores from the Ross Sea in Antarctica were taken from grounding zone wedges, topsets, and foresets, which demonstrated the presence of six facies with distinct depositional processes in subglacial and glacial proximal environments (Prothro *et al.*, 2018). Prothro *et al.* (2018) conducted research on

these cores using methods such as grain size analysis, geotechnical properties, and micropaleontology. These techniques improved the distinction between ice-proximal diamictos and subglacial diamictos (Prothro *et al.*, 2018).

The core sections recovered from 34R, 35R, and 36R, all below 280 mbsf, are predominantly composed of diamictites and mudstones. These sections exhibit characteristics of glacial distal environments in proximity to the calving zone and open marine environments (Prothro *et al.*, 2018). The glaciomarine origin is evident in the massive, laminated, and weakly bioturbated muds with high IRD content that dominate these sediments (Figure 4). Well-sorted coarse silt can be evidence of suspension settling and a less dynamic depositional environment, which is visible in the core sections deeper than 280 mbsf. The sediment is better sorted than other samples in the dataset. Figure 6 shows that sediment in these cores below 280 mbsf was coarser than the upper samples in the dataset as well. As 34R, 35R, and 36R at Site 1097 show increased grain size, we can infer that the Early Pliocene conditions and increased susceptibility of the APIS to climate change could have induced ice shelf collapse.

The most comparable facies for these core sections is Facies 5 of Prothro *et al.* (2018), which has strong characteristics of an open marine environment. These facies are primarily a result of suspension settling, with coarser materials deposited by floating icebergs or sea ice. As IRD flux increases, mud with isolated dropstones can transition to massive diamictite when enough clasts accumulate (Prothro *et al.*, 2018). Conversely, decreased IRD deposition can cause massive diamictite to become mudstone with isolated dropstones due to the reduced clast concentration, suggesting large meltwater influxes, suspended sediment settling, and iceberg calving. Furthermore, sand in open marine and glacial distal environments can be interpreted as ice-rafted debris. These environments are sometimes referred to as “compound glacial marine”



due to their composition, which is a combination of fine sediment and IRD. The sand percentage and mud content provide useful indicators of glacial proximal or ice-distal environments. A soft glacial marine drape with a poorly sorted structure that resembled the texture of its basal debris source was observed at distances of up to 300 m from the GL. This drape was made up of clast-rich sandy mud and diamicton (Smith *et al.*, 2019).

Three samples were examined from core 36R, and particle size analysis and sediment facies can be interpreted as ice shelf collapse, a phenomenon during glacial retreat during warm periods. The sediment facies were sandy mud, meaning that each sample contained 20% or more sand. Additionally, core section 36R alternated between massive diamictite and deformed mud facies. The high sand content and sediment facies of these samples are similar to the geological signature of ice shelf collapse, which is characterized by a mixture of marine and aeolian sediment (Smith *et al.*, 2019). Ice shelves contain a moderate amount of supraglacial sediments, which, through hydrofracturing, can be exported to the seafloor during ice shelf collapse. Sediments resulting from ice shelf collapse are typically dominated by muddy sand, sand, and diamictite, which are coarse-grained. This could explain the increase in median grain size with depth, as shown in Figure 6. The highest plotted samples in Figure 7 were subsamples from core 36R, which had the highest sand:clay ratio in the data set. Ice shelf collapse generally occurs in ice distal environments, such as open marine, calving zones, and calving lines, which are depicted by the 36R subsamples (Smith *et al.*, 2019). The geological signature of ice shelves has been difficult to prove until recently, and much is still unknown about its defining characteristics. However, the 36R facies and grain size analysis are consistent with an ice shelf collapse signature.

The particle size data suggests that the average grain size increased with depth and that uniformity decreased as depth increased. Moreover, the average grain size did not linearly progress, and there were multiple fluctuations, as the samples were selected to capture the variability in the facies. A change in uniformity could indicate a change in the depositional environment or a major depositional event. A change in uniformity is evident around 280 meters below the seafloor (mbsf). A gravity flow or large influx of meltwater could have caused a peak in the uniformity, meaning an interval of poor sorting, at ~275 mbsf. An ice shelf collapse could also deposit a large influx of poorly sorted sediment, but that could only happen during a period of glacial retreat (Davies *et al.*, 2012). The glacial advance can be interpreted in core sections through the presence of burrowed, graded, and stratified diamictite, occasionally accompanied by burrowed muds (Figure 4). Stratified and graded diamictites are predominantly interpreted as subaqueous sediment gravity flows. Prothro *et al.* (2018) identified these characteristics in Facies 1 and 2. Facies 1 represents glacial till, while Facies 2 consists primarily of grounding zone debris flow. Both facies contain reworked foraminifera and lack a pristine record of biogenic material, similar to the Pliocene sediments found in the uppermost core sections at Site 1097. These facies classifications provide insight into the depositional processes that occurred during the glacial advance, which is depicted by core sections 26R, 27R, 28R, 32R, and 33R.

Glacial proximal sedimentary facies indicate the presence of stable ice sheets in close proximity to the drill site. Results from samples from Cores 26R, 27R, 28R, 32R, and 33R, above 280 mbsf, are consistent with this environment, which comprises over 60% of the core sections sampled (Eyles *et al.*, 2001). Sediment deposition occurs from basal melting of the ice sheet and shelf currents. Whether IODP Site 1097 cores were taken from GZW's topsets or foresets is not known. However, core descriptions are indicative of three of the six facies

described in Prothro *et al.* (2018). Facies 1-2 are consistently poorly sorted throughout the core sections, with a sandy silt matrix and occasional pebbles. The majority of the samples analyzed from Site 1097 had a sandy silt composition, indicating fine-grained sediment throughout core sections (Figure 6). Some samples contained a high sand content, indicating the deposition of aeolian sediment or IRD. The characteristics of coarse-grained material vary depending on the mechanisms that deposit them. In a glacial proximal environment, aeolian sediment can result from hydrofracturing of ice shelves and the export of aeolian sediment to the sea floor (Smith *et al.*, 2019). Sediment-rich meltwater and shelf currents can also carry coarse grains such as sand toward the grounding line. In a glacial distal and open marine environment, sediment deposition may occur from the calving of icebergs, rainout from floating ice, and ice sheet collapse, although this is not a common phenomenon.

The geological data and facies suggest that there was glacial retreat in the Early Pliocene, which included iceberg calving at a high rate, with periods of low activity and suspension settling. The Early Pliocene alternated between a calving zone and an open marine environment. After the deposition of sediments recovered in core 34R, the Antarctic ice sheet began to advance, significantly reducing the area of the cavity beneath the APIS as the ice sheet began to ground. The environment quickly transitioned to an ice-proximal environment and glacial advance proceeded. Further evidence supporting the advance of the ice sheet is that sediment recovered in core 26R, the shallowest core examined in this study, was massive diamictite facies, strongly indicating a subglacial environment, which means the ice sheet continued to expand.

Glacial unconformities are apparent in seismic data beneath the thick Pliocene strata on the Antarctic continental shelves, providing evidence of ice sheet advance despite the warm

climate in the Pliocene. Peak eustatic low stands coupled with  $^{18}\text{O}$  enrichments in the Early Pliocene indicate that the global ice sheet volume was 18% larger than it is today (Bart, 2001). Furthermore, 30 unconformities were identified by Bart (2001), suggesting that the APIS extended past the continental shelf more than 30 times in the Pliocene. This exceeds the 12 unconformities that occurred in the Miocene record, which were induced by the APIS. The advance of the APIS is also supported by sediments in large drift deposits located adjacent to the continental rise, indicating multiple phases of advance and retreat of grounded ice sheets across the shelf.

### **Other Reconstructions of the Pliocene APIS**

The study conducted on James Ross Island, located off the coast of the Antarctic Peninsula, utilized cosmogenic  $^3\text{He}$  exposure dating to determine the thickness of the ice sheet (Johnson *et al.* 2009). While an exact measurement of ice sheet thickness alone could not be determined, Johnson *et al.* (2009) inferred that the ice sheet was at least 8 meters thick during this period. This is because cosmic rays cannot penetrate snow thicker than 8 meters. The presence of striations, hollows, and eroded bedrock and substrate in the area of Patalamon Mesa also provided insight into ice thickness parameters. These geological features indicated a minimum ice sheet thickness of 45 to 200m. Only an ice sheet of that size could leave such a geological imprint. This size was calculated using snow accumulation rates, flow speed, and geothermal heat flux. Samples collected above 600 m above sea level indicated that the APIS was at least 600 m thick over the last 4.69 million years. This is in agreement with the findings that the APIS remained relatively stable during the early Pliocene, as supported by geochemical data derived from ICP-MS analysis. Although the grounding line of the Marguerite Ice Stream did retreat, this study's findings suggest that the ice sheet was rather stable.

The lithofacies analysis of the continental shelf can help determine ice-proximal depositional environments throughout the geological timescale. Analyzing cores from Site 1097 could provide evidence of ice shelf collapse. However, there is a lack of understanding of the geological imprint of ice shelves, and the processes that occur in their vicinity are still poorly understood. Breakup of ice shelves has been linked to climate changes for over two centuries, caused by hydrofracture from water-filled crevasses, which was also the same driving force behind the ice sheet breakdown in the previously mentioned model. CDW upwelling is a key driver of ice shelf retreat today and it is possible that it could have affected ice sheet dynamics in the Pliocene as well. The climate variable that separates the Pliocene from today is approximately 2 degrees C of warming, and CO<sub>2</sub> levels have been said to be around the same mark as the present day at 400 ppm. Recent advancements in understanding the geological signatures of ice shelves since the lithostratigraphy of Site 1097 was last examined 20 years ago suggest that further research in this area is warranted.

### **CONCLUSION**

The core samples obtained from ODP Site 1097 provided evidence that the APIS retreated and advanced during the Early Pliocene. Figure 11 displays evidence of this pattern, with multiple core sections alternating back and forth from two facies, notably cores 27R and 36R. Several ice-sheet models suggest that the APIS would be reduced to small local ice caps during Pliocene warming events, such as the one that occurred in the Early Pliocene. However, geophysical and marine geological studies conducted on Site IODP 1097 and its three counterparts (1095, 1096, 1101) strongly suggest that the APIS was present during the Neogene period, indicated by seismic reflectors known as glacial unconformities. Unconformities found in

seismic data on the Antarctic Peninsula continental shelf suggest that approximately 30 advances and retreats occurred during interglacial and glacial cycles, each lasting about 40,000 years.

The core samples from sections 34R, 35R, and 36R contained strong evidence of retreat, indicated by sedimentary facies and particle size analysis. The dominant facies were burrowed mud with dropstones and diamict, which can be interpreted as ice distal environments ranging from sub-ice shelf to open marine environments. These ice distal environments were prevalent during the Early Pliocene due to temperatures that were 2-3 degrees higher than they are today. Conversely, shallow cores examined at sections 26R, 27R, 28R, 32R, and 33R indicated more of an ice-proximal environment, an indication of glacial advance during the Early Pliocene.

Although there were strong indications of glacial advance and retreat, geochemical data suggest that the APIS was still a rather stable ice sheet during the Pliocene. The low CIA values point to a cool, dry climate and sediment with a strong glacial imprint. No significant changes in the source material are shown by trace element and REE ratios. The data derived from this research is critical in understanding how the cryosphere responds to rising CO<sub>2</sub> and temperature. The APIS dynamics during this period are not a blueprint for all ice sheets in the future, but they do help us understand the behavior of ice sheets better under extreme atmospheric conditions. To predict and prepare for the cryosphere's response in the foreseeable future, we must understand the effects of Earth's elevated greenhouse on the climate in both interglacial and glacial periods.

The APIS dynamics during the Pliocene are a key indicator of the ice sheet's foreseeable future if global temperatures continue to rise, the focal point of this study. Geological data suggest that the APIS will remain intact if global temperatures remain what they are today. Even though it may have increased sensitivity to climate change, the APIS may be as resilient to warming as the East Antarctic Ice Sheet. However, continued warming will cause substantial

glacial retreat, induce ice shelf collapse, and lead to calving of icebergs and hydrofracturing, as temperatures continue to rise.

### **DATA STATEMENT**

The data produced as part of this thesis will be available in the U.S. Antarctic Program Data

Center: <https://www.usap-dc.org/>

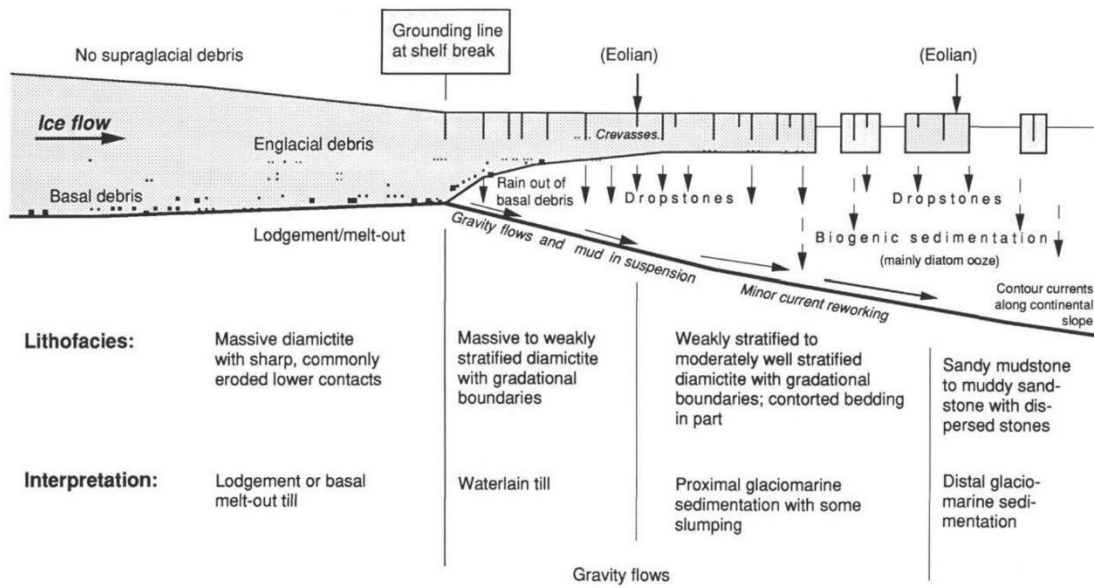


Figure 1: Sedimentary facies associated with an Antarctic ice shelf (Hambrey et al., 1991).



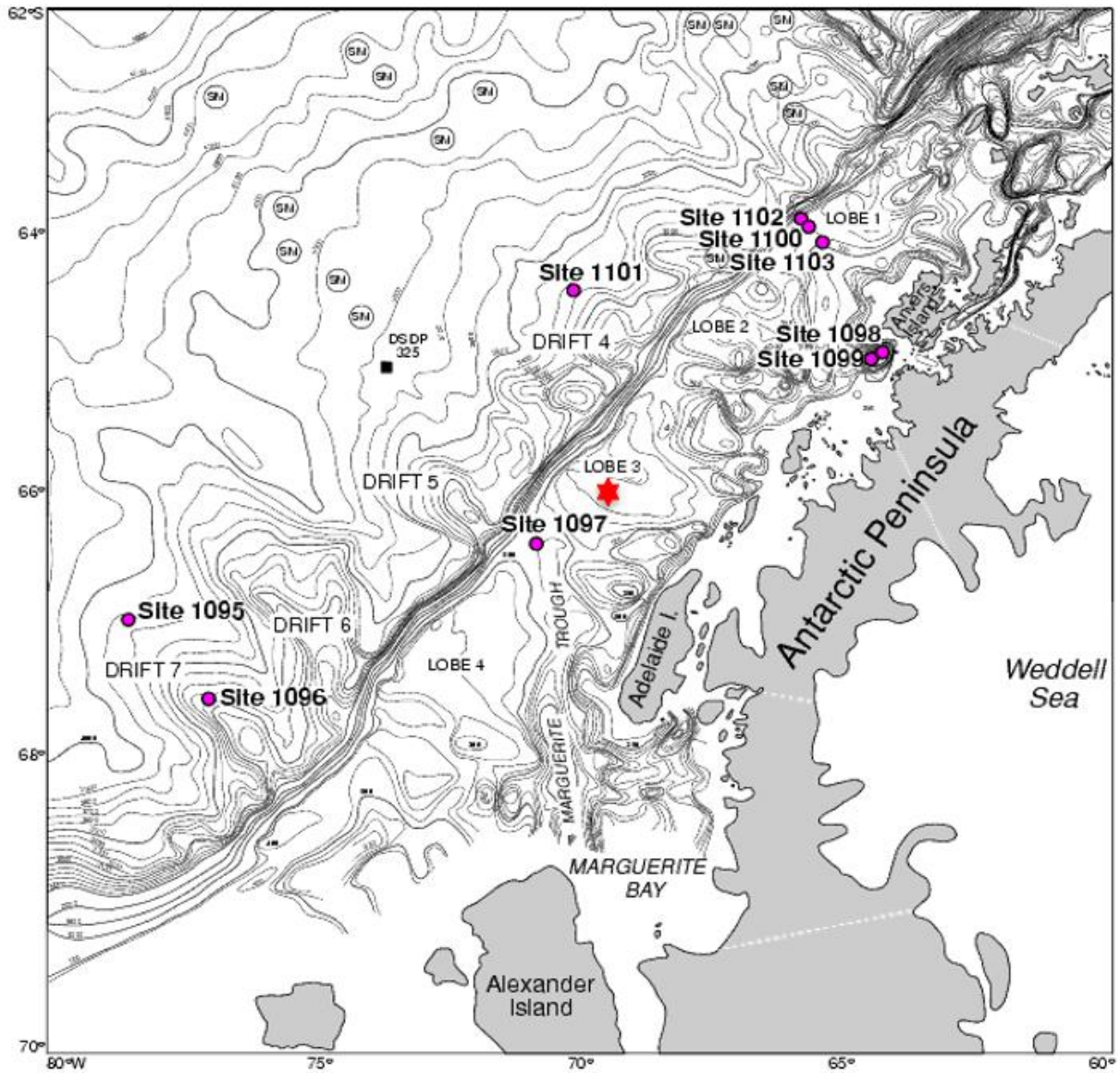


Figure 2: ODP Site 1097 studied in this thesis is located at the seaward end of Marguerite Trough, Antarctica (Barker et al., 1999).

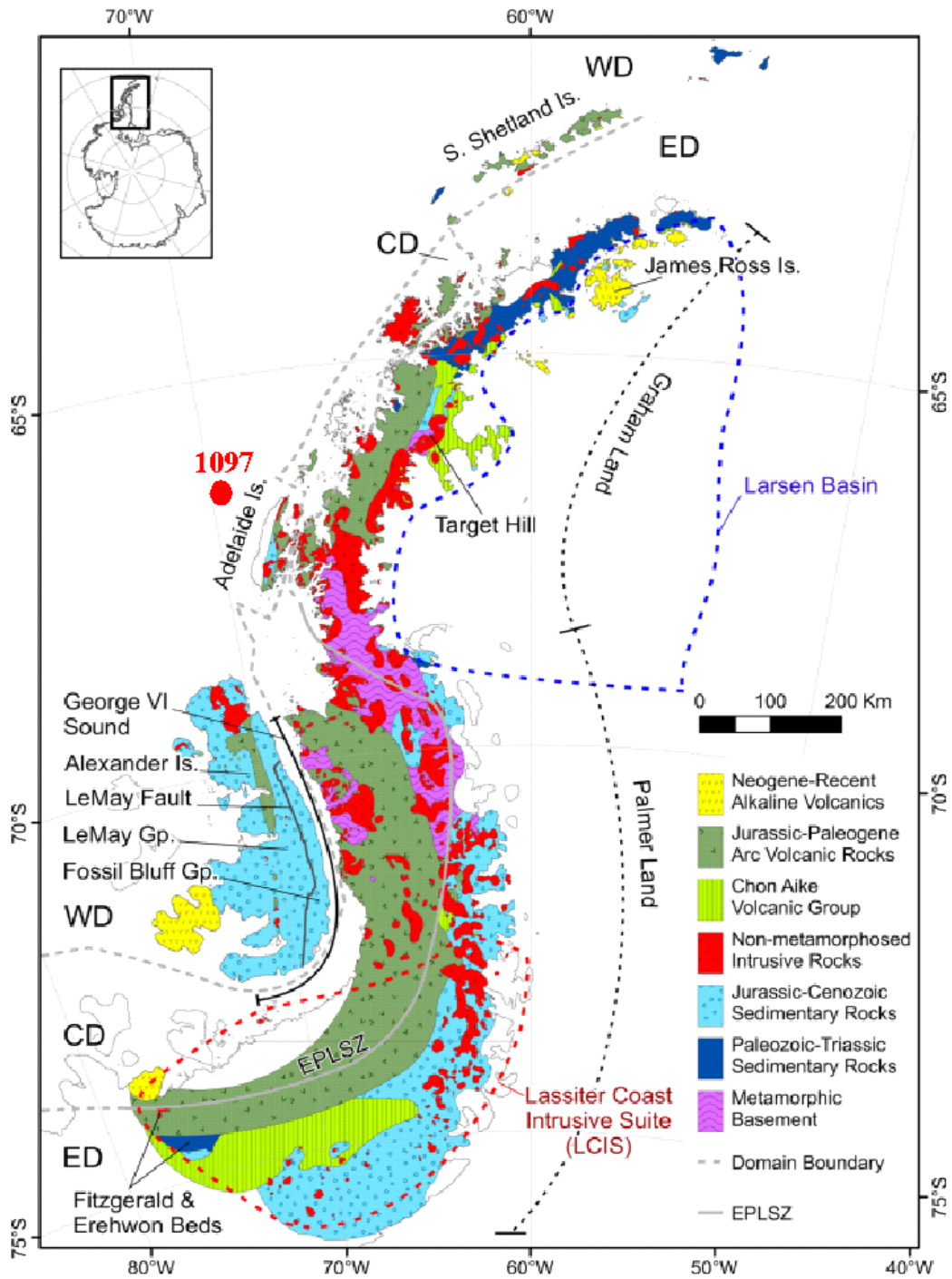


Figure 3: Geological map of the Antarctic Peninsula, showing the distribution of the principal geological units defined in the text (Burton-Johnson & Riley, 2015).

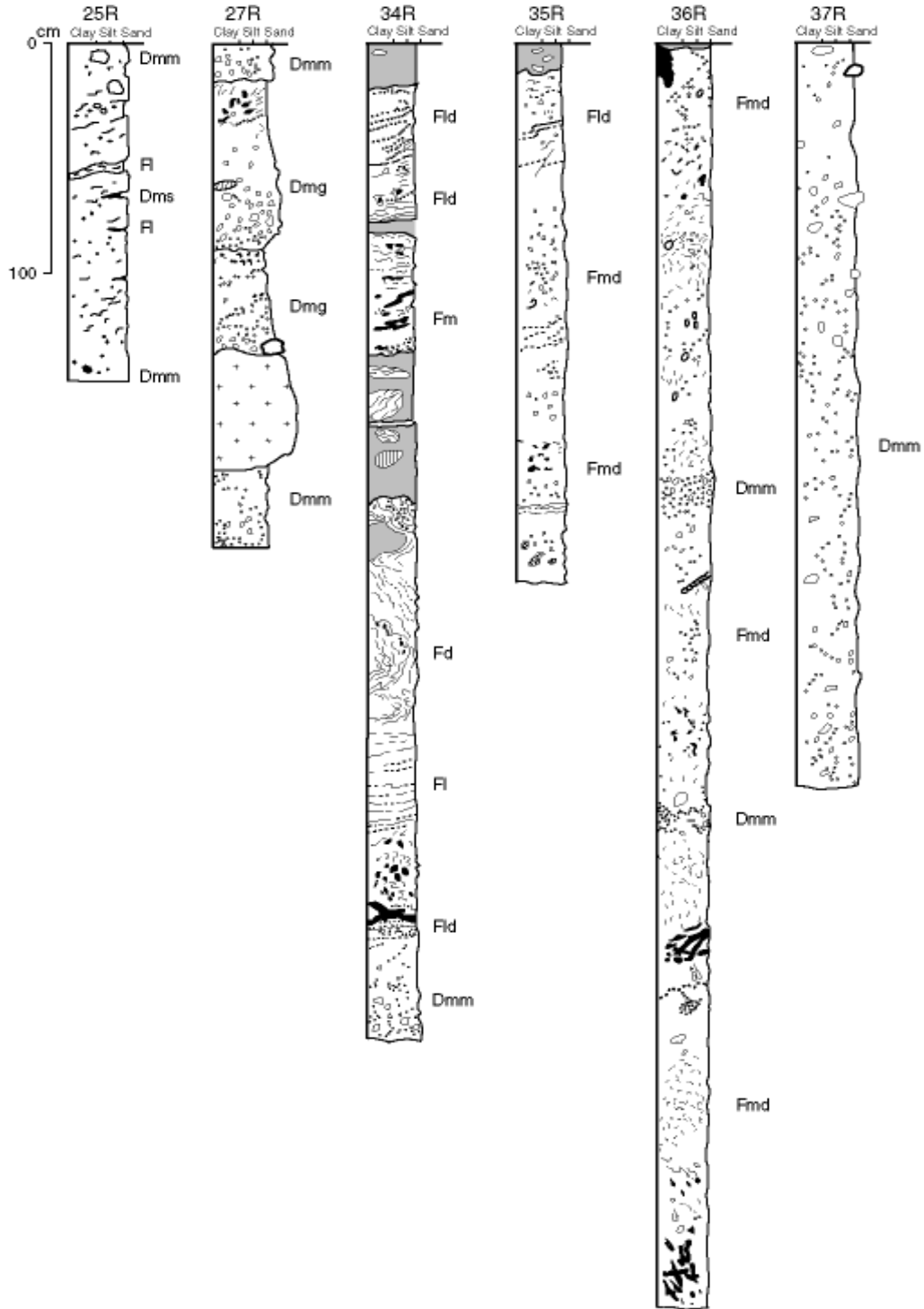


Figure 4: Interpreted Core section IODP Site 1097 Leg 178 lithofacies for Cores 25R through 37R (Barker et al., 1999).

Fmd = Mudstone massive with dropstones, Dmm = Diamict massive matrix-supported, Fd = Mudstone deformed, Fm = Mudstone massive, Fld = Mudstone Laminated with dropstones, Fl = Mudstone laminated, Dmg = Diamict degraded.

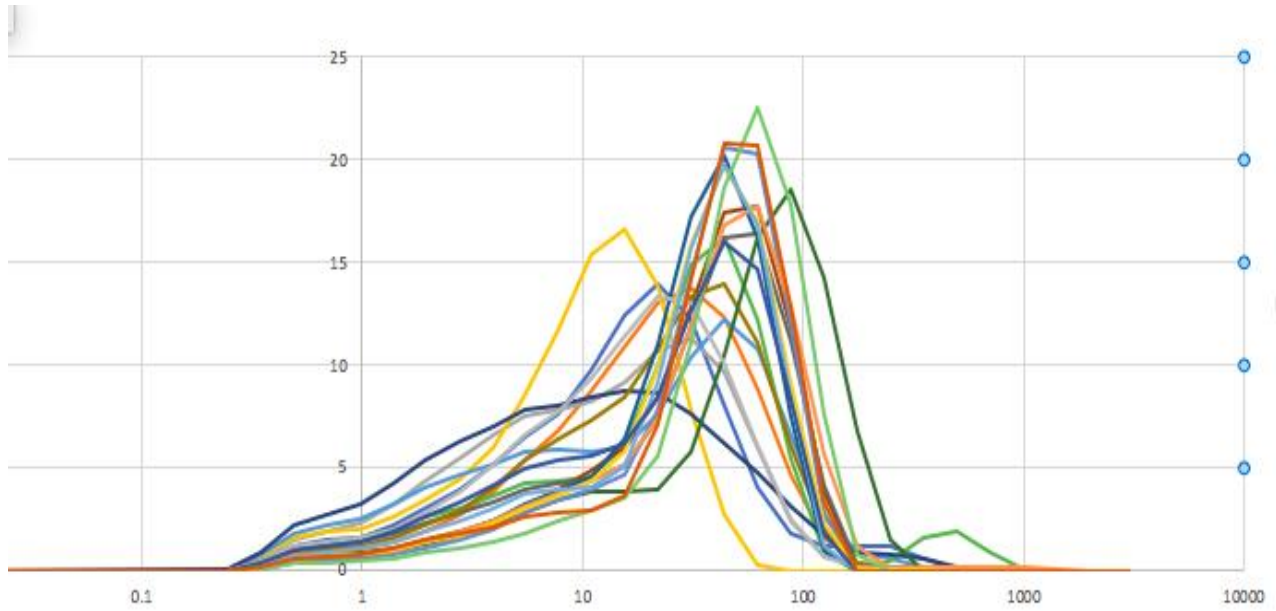


Figure 5: Grain Size Distribution of 20 core samples. The horizontal axis refers to particle diameter in micrometer. The vertical axis shows volume percent in each half Phi bin.

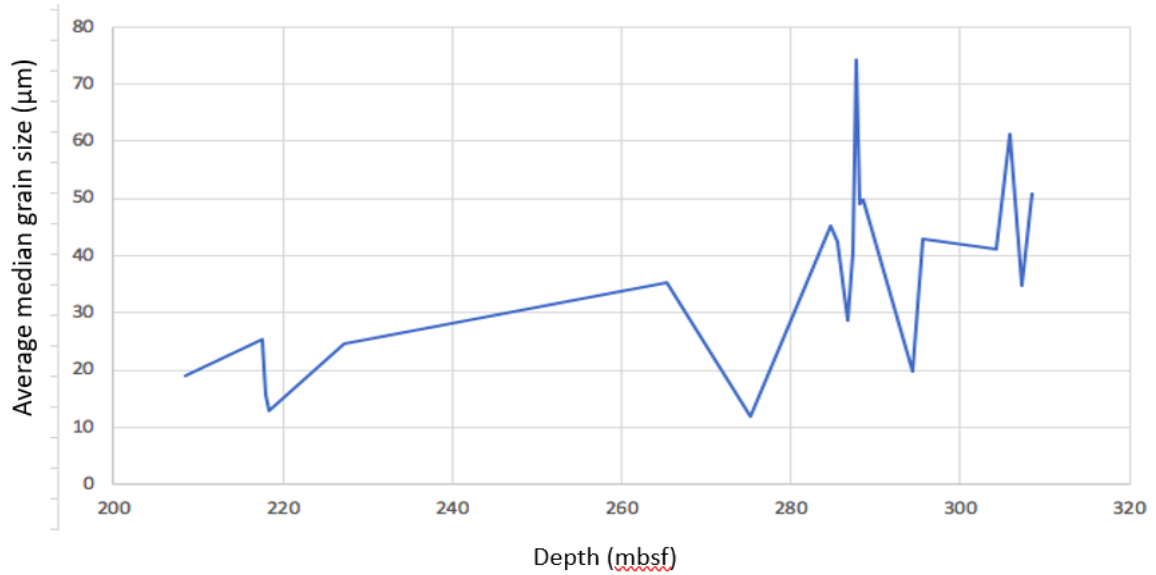


Figure 6: Median grain size ( $\mu\text{m}$ ) with depth in meter below sea floor (mbsf).

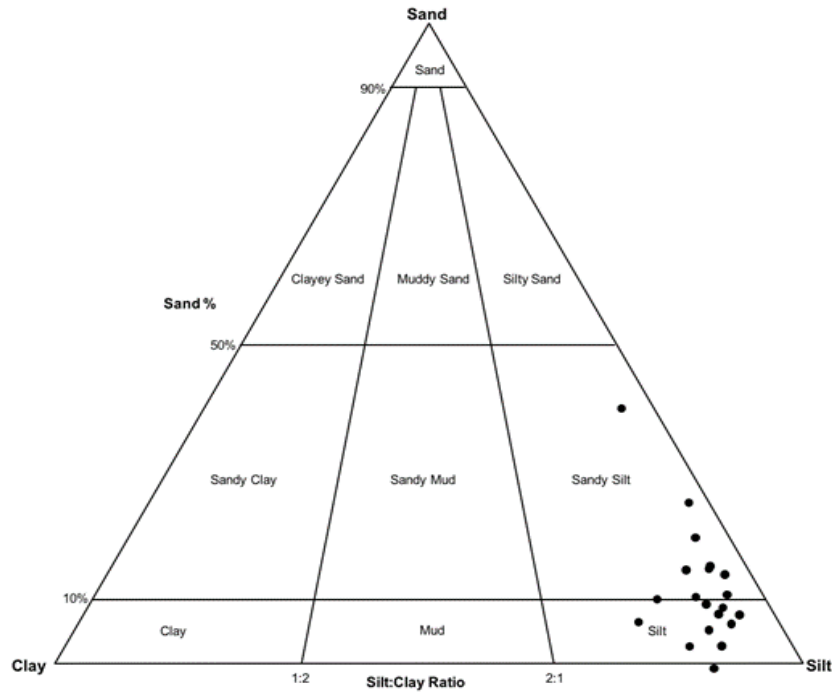


Figure 7: The silt to clay ratio of all 20 samples studied.

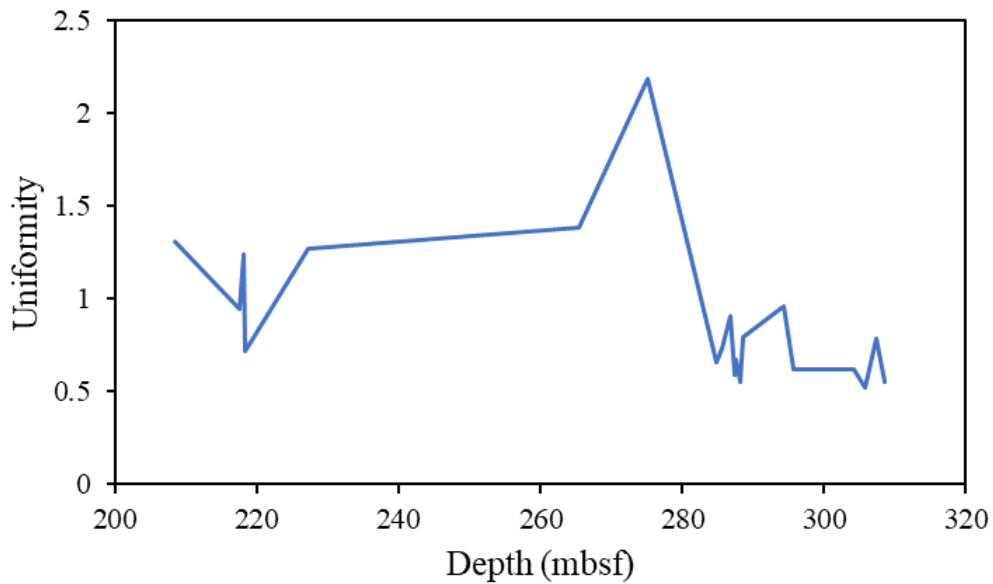


Figure 8: Uniformity is indicated on the x axis and y axis core depth in meters below the seafloor calculated as the diameter greater than that of 60% of particles divided by the diameter greater than 10% of particles (Passchier et al., 2018). The range is from 208.5-308.5 mbsf.

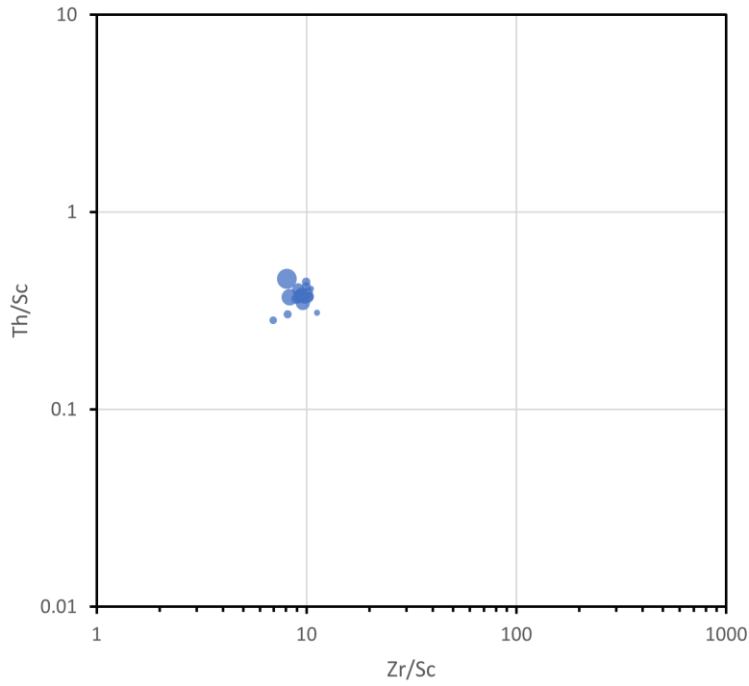


Figure 9: A plot of Th/Sc versus Zr/Sc ratio of the 20 samples taking from cores of IODP 1097 (McLennan et al., 1993).

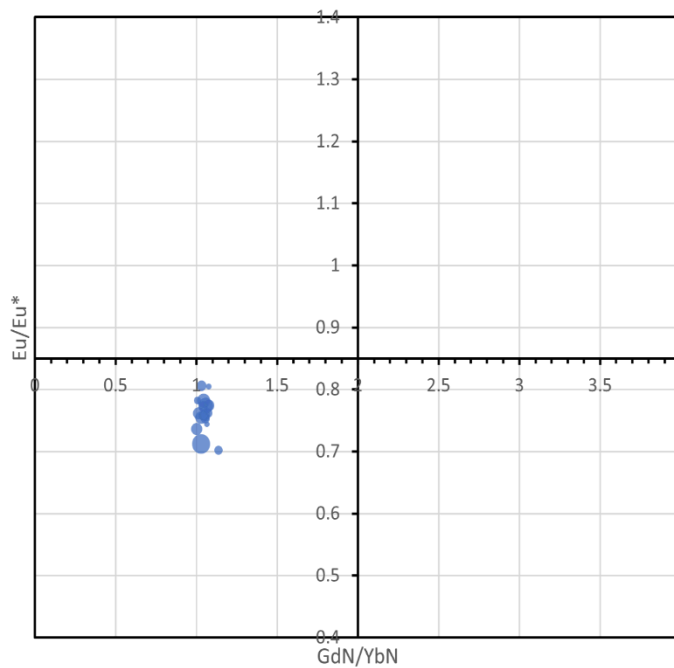


Figure 10: Plot of Gd<sub>N</sub>/Yb<sub>N</sub> versus Eu/Eu\* ratio of the 20 samples that were examined from ODP Site 1097 (McLennan et al., 1993).

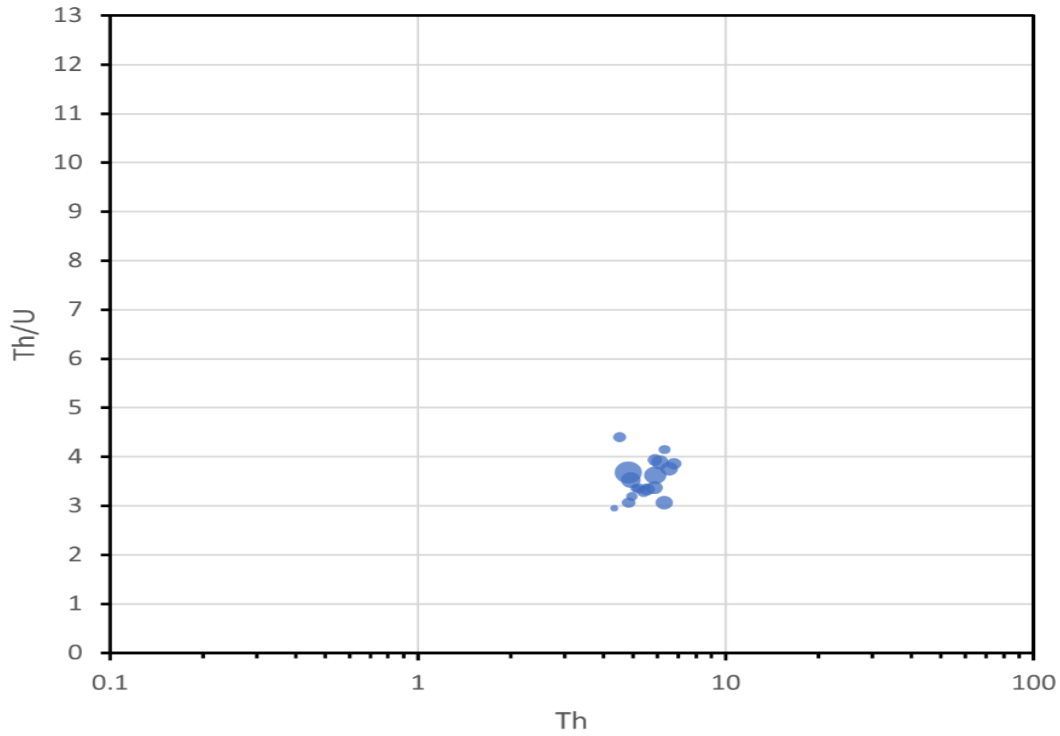


Figure 11: Th/U versus Th plot ratio of 20 samples that were examined from Site IODP Site 1097 (McLennan et al., 1993).

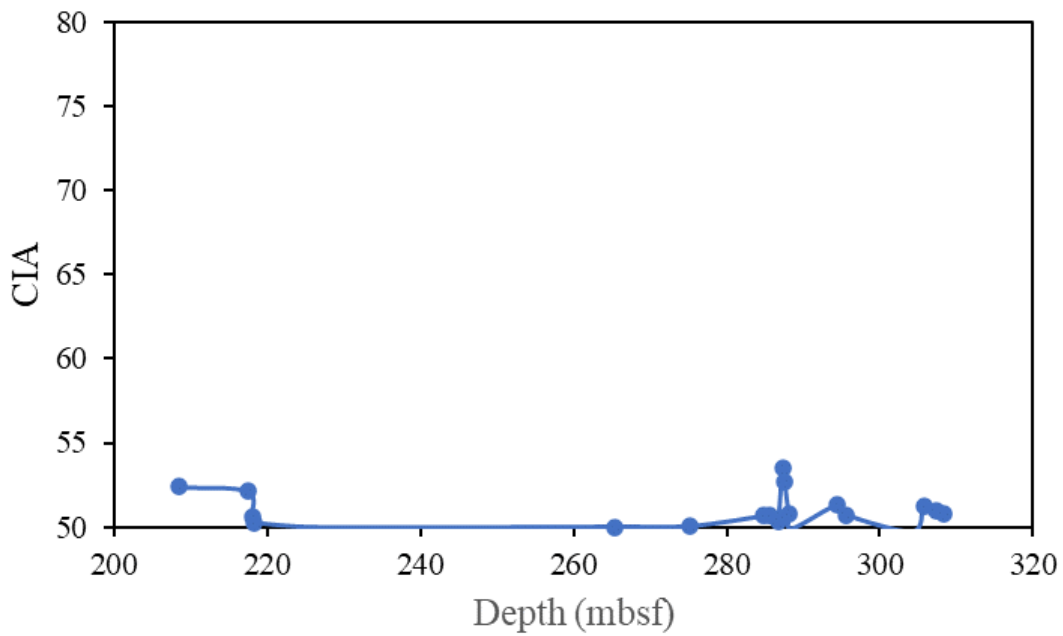


Figure 12: The vertical axis is CIA values of samples of IODP 1097, and the horizontal axis pertains to mbsf of each sample.

**REFERENCES**

- Barker, P. F., & Camerlenghi, A. (2002). Glacial history of the Antarctic Peninsula from Pacific margin sediments. In *Proceedings of the Ocean Drilling Program. Scientific Results* (Vol. 178, pp. 1-40).
- Barker, P.F., Camerlenghi, A., Acton, G.D., and Ramsay, A.T.S. (1999). *Proceedings of the Ocean Drilling Program, Scientific Results* (Volume 178), [CDROM], Ocean Drilling Program, Texas A&M University.
- Bart, P.J., and Anderson, J.B. (1997). Grounding Zone Wedges on the Antarctic Continental Shelf, Antarctic Peninsula. In T.A. Davies, T. Bell et al. (Eds.), *Glaciated Continental Margins* (pp. 96-97). Dordrecht, Springer Netherlands. [https://doi.org/10.1007/978-94-011-5820-6\\_36](https://doi.org/10.1007/978-94-011-5820-6_36)
- Blott, S. J., & Pye, K. (2001). GRADISTAT: a grain size distribution and statistics package for the analysis of unconsolidated sediments. *Earth surface processes and Landforms*, 26(11), 1237-1248. <https://doi.org/10.1002/esp.261>.
- Burton-Johnson, A., & Riley, T. R. (2015). Autochthonous v. accreted terrane development of continental margins: a revised in situ tectonic history of the Antarctic Peninsula. *Journal of the Geological Society*, 172(6), 822-835. <https://doi.org/10.1144/jgs2014-110>.
- Cook, A. J., Fox, A. J., Vaughan, D. G., & Ferrigno, J. G. (2005). Retreating glacier fronts on the Antarctic Peninsula over the past half-century. *Science*, 308(5721), 541-544. <https://doi.org/10.1126/science.1104235>.
- Crampton-Flood, E. D., Peterse, F., Munsterman, D., & Damsté, J. S. S. (2018). Using tetraether lipids archived in North Sea Basin sediments to extract North Western European Pliocene



continental air temperatures. *Earth and Planetary Science Letters*, 490, 193-205.

<https://doi.org/10.1016/j.epsl.2018.03.030>.

Davies, B. J., Hambrey, M. J., Smellie, J. L., Carrivick, J. L., & Glasser, N. F. (2012). Antarctic Peninsula ice sheet evolution during the Cenozoic Era. *Quaternary Science Reviews*, 31, 30-66. <https://doi.org/10.1016/j.quascirev.2011.10.012>.

DeConto, R. M., & Pollard, D. (2016). Contribution of Antarctica to past and future sea-level rise. *Nature*, 531(7596), 591-597. <https://doi.org/10.1038/nature17145>.

Eyles, N., Daniels, J., Osterman, L. E., & Januszczak, N. (2001). Ocean Drilling Program Leg 178 (Antarctic Peninsula): sedimentology of glacially influenced continental margin topsets and foresets. *Marine Geology*, 178(1-4), 135-156. [https://doi.org/10.1016/s0025-3227\(01\)00184-0](https://doi.org/10.1016/s0025-3227(01)00184-0).

Fedo, C. M., Wayne Nesbitt, H., & Young, G. M. (1995). Unraveling the effects of potassium metasomatism in sedimentary rocks and paleosols, with implications for paleoweathering conditions and provenance. *Geology*, 23(10), 921-924.

[https://doi.org/10.1130/00917613\(1995\)023<0921:uteopm>2.3.co;2](https://doi.org/10.1130/00917613(1995)023<0921:uteopm>2.3.co;2).

Guo, Q., Xiao, W., Windley, B. F., Mao, Q., Han, C., Qu, J., ... & Yong, Y. (2012). Provenance and tectonic settings of Permian turbidites from the Beishan Mountains, NW China: implications for the Late Paleozoic accretionary tectonics of the southern Altaids. *Journal of Asian Earth Sciences*, 49, 54-68. <https://doi.org/10.1016/j.jseaes.2011.03.013>

Hambrey, M.J., Ehrmann, W.U., & Larsen, B. (1991). Cenozoic glacial record of the Prydz Bay continental shelf, East Antarctica. In: J. Barron, B. Larsen et al. (Eds.), *Proceedings of the Ocean Drilling Program, Scientific Results* (Vol. 119, pp: 77-132). Ocean Drilling Program, College Station, TX. <https://doi.org/10.2973/odp.proc.sr.119.200.1991>

- Johnson, J. S., Smellie, J. L., Nelson, A. E., & Stuart, F. M. (2009). History of the Antarctic Peninsula Ice Sheet since the early Pliocene—evidence from cosmogenic dating of Pliocene lavas on James Ross Island, Antarctica. *Global and Planetary Change*, 69(4), 205-213. <https://doi.org/10.1016/j.gloplacha.2009.09.001>.
- Jordan, T. A., Riley, T. R., & Siddoway, C. S. (2020). The geological history and evolution of West Antarctica. *Nature Reviews Earth & Environment*, 1(2), 117-133. <https://doi.org/10.1038/s43017-019-0013-6>.
- Konert, M., & Vandenberghe, J. E. F. (1997). Comparison of laser grain size analysis with pipette and sieve analysis: a solution for the underestimation of the clay fraction. *Sedimentology*, 44(3), 523-535. <https://doi.org/10.1046/j.1365-3091.1997.d01-38.x>.
- McKay, R. M., De Santis, L., Kulhanek, D. K., Ash, J. L., Beny, F., Browne, I. M., ... & Xiong, Z. (2019). Expedition 374 summary. *Proceedings of the International Ocean Discovery Program*.
- McLennan, S. M. (2018). Rare earth elements in sedimentary rocks: influence of provenance and sedimentary processes. In *Geochemistry and mineralogy of rare earth elements* (pp. 169-200). De Gruyter. <https://doi.org/10.1515/9781501509032-010>
- McLennan, S. M., Hemming, S., McDaniel, D. K., & Hanson, G. N. (1993). Geochemical approaches to sedimentation, provenance, and tectonics. *Special Papers-Geological Society of America*, 21-40. <https://doi.org/10.1130/SPE284-p21>
- Murray, R. W., Miller, D. J., & Kryc, K. A. (2000). Analysis of major and trace elements in rocks, sediments, and interstitial waters by inductively coupled plasma–atomic emission spectrometry (ICP-AES). Ocean Drilling Program.

- Nesbitt, H., & Young, G. M. (1982). Early Proterozoic climates and plate motions inferred from major element chemistry of lutites. *nature*, 299(5885), 715-717.  
<https://doi.org/10.1038/299715a0>.
- Passchier, S., Ciarletta, D. J., Henao, V., & Sekkas, V. (2018). Sedimentary processes and facies on a high-latitude passive continental margin, Wilkes Land, East Antarctica. *Geological Society, London, Special Publications*, 475(1), 181-201. <https://doi.org/10.1144/SP475.3>
- Passchier, S., Ciarletta, D. J., Miriagos, T. E., Bijl, P. K., & Bohaty, S. M. (2017). An Antarctic stratigraphic record of stepwise ice growth through the Eocene-Oligocene transition. *Bulletin*, 129(3-4), 318-330. <https://doi.org/10.1130/B31482.1>
- Potter, P. E., Maynard, J. B., & Depetris, P. J. (2005). *Mud and mudstones: Introduction and overview*. Springer Science & Business Media, Springer Berlin, Heidelberg.  
<https://doi.org/10.1007/b138571>
- Prothro, L. O., Simkins, L. M., Majewski, W., & Anderson, J. B. (2018). Glacial retreat patterns and processes determined from integrated sedimentology and geomorphology records. *Marine Geology*, 395, 104-119. <https://doi.org/10.1016/j.margeo.2017.09.012>.
- Reese, R., Garbe, J., Hill, E. A., Urruty, B., Naughten, K. A., Gagliardini, O., ... & Winkelmann, R. (2022). The stability of present-day Antarctic grounding lines—Part B: Possible commitment of regional collapse under current climate. *The Cryosphere Discussions*, 1-33.  
<https://doi.org/10.5194/tc-2022-105>
- Robinson, L. F., Noble, T. L., & McManus, J. F. (2008). Measurement of adsorbed and total  $^{232}\text{Th}/^{230}\text{Th}$  ratios from marine sediments. *Chemical Geology*, 252(3-4), 169-179.  
<https://doi.org/10.1016/j.chemgeo.2008.02.015>

Shepherd, A., Wingham, D., & Rignot, E. (2004). Warm ocean is eroding West Antarctic ice sheet. *Geophysical Research Letters*, *31*(23). <https://doi.org/10.1029/2004GL021106>

Shipboard Scientific Party. (1999). Leg 181 Summary: Southwest Pacific Paleooceanography. In R.M. Carter, I.N. McCave et al. (Eds.), *Proceedings of the Ocean Drilling Program, Initial Reports* (pp. 1-80). Ocean Drilling Program, Texas A&M University.

Smellie, J. L., Haywood, A. M., Hillenbrand, C. D., Lunt, D. J., & Valdes, P. J. (2009). Nature of the Antarctic Peninsula Ice Sheet during the Pliocene: Geological evidence and modelling results compared. *Earth-Science Reviews*, *94*(1-4), 79-94.  
<https://doi.org/10.1016/j.earscirev.2009.03.005>.

Smith, J. A., Graham, A. G., Post, A. L., Hillenbrand, C. D., Bart, P. J., & Powell, R. D. (2019). The marine geological imprint of Antarctic ice shelves. *Nature Communications*, *10*(1), 5635.  
<https://doi.org/10.1038/s41467-019-13496-5>.

Taylor, S. R., & McLennan, S. M. (1985). The continental crust: its composition and evolution. Blackwell, Oxford, 1-312.

Thiry, M. (2000). Palaeoclimatic interpretation of clay minerals in marine deposits: an outlook from the continental origin. *Earth-Science Reviews*, *49*(1-4), 201-221.  
[https://doi.org/10.1016/S0012-8252\(99\)00054-9](https://doi.org/10.1016/S0012-8252(99)00054-9)

Vaughan, D. G., Marshall, G. J., Connolley, W. M., Parkinson, C., Mulvaney, R., Hodgson, D. A., ... & Turner, J. (2003). Recent rapid regional climate warming on the Antarctic Peninsula. *Climatic change*, *60*, 243-274. <https://doi.org/10.1023/A:1026021217991>